

# Chemical doping-induced gap opening and spin polarization in graphene

I. Zanella<sup>1</sup>, S. Guerini<sup>2</sup>, S. B. Fagan<sup>3</sup>, J. Mendes Filho<sup>1</sup>, A. G. Souza Filho<sup>1\*</sup>

<sup>1</sup>*Departamento de Física, Universidade Federal do Ceará,  
CP 6030, CEP 60455-900, Fortaleza, CE, Brazil*

<sup>2</sup>*Departamento de Física, Universidade Federal  
do Maranhão, 65080-040, São Luis, MA, Brazil*

<sup>3</sup>*Área de Ciências Naturais e Tecnológicas,  
Centro Universitário Franciscano, CEP 97010-032, Santa Maria, RS, Brazil*

(Dated: October 27, 2018)

## Abstract

By using first principles calculations we report a chemical doping induced gap in graphene. The structural and electronic properties of  $\text{CrO}_3$  interacting with graphene layer are calculated using ab initio methods based on the density functional theory. The  $\text{CrO}_3$  acts as an electron acceptor modifying the original electronic and magnetic properties of the graphene surface through a chemical adsorption. The changes induced in the electronic properties are strongly dependent of the  $\text{CrO}_3$  adsorption site and for some sites it is possible to open a gap in the electronic band structure. Spin polarization effects are also predicted for some adsorption configurations.

PACS numbers: 73.22.-f, 73.20.Hb, 73.61.Wp

---

\* Corresponding author - E-mail: agsf@fisica.ufc.br

Nanostructured carbon-based materials exhibit remarkable electronic properties making them promising materials to be used in a wide range of technological applications, including a possible carbon-based electronics in a near future [1, 2]. Graphene, a single atom thick layer, is considered the mother structure of all  $sp^2$  nanostructured carbon (such as fullerenes, carbon nanotubes and ribbons) and its electronic structure has been theoretically investigated since 1947 [3]. A breakthrough in carbon science was the recent observation of graphene single layer that was obtained by micromechanical cleavage of graphite [4, 5]. The linear electronic band structure at the corner of the Brillouin zone where there is a band crossing between the conduction and valence bands cross is responsible for striking physical properties not observed in any other material such as ballistic transport [5], and quantum Hall effect at room temperature [6, 7] and typical relativistic phenomena such as Berry's phase and Klein paradox as a consequence of massless Dirac Fermions. The chemical stability, scalability and the complete compatibility of graphene with current semiconductor technology pave the way for the next generation of devices operating with a carbon based electronic.

The possibility of tailoring the electronic properties (type and number of carriers) of graphene is important not only for basic studies but also for further optimization of their applications mainly as nanoscale based-sensors or spin filter devices [8, 9, 10, 11, 12]. The electronic properties can be tuning either by carrying out donor/acceptor doping experiments or by applying a gate bias voltage [10, 13]. The electric field polarization and the electronegativity of the doping species modify the carrier type (electron or hole) and carrier concentration at the Dirac point affecting the electronic structure and consequently the transport properties of graphene to a large extent. In this regard, a recent experimental work by Schedin et al. [10] fabricated and operated a single molecule based sensor. The authors show, through measurements of quantum Hall effect, that  $\text{NO}_2$ ,  $\text{H}_2\text{O}$  and iodine acts as electron acceptors whereas  $\text{NH}_3$ ,  $\text{CO}$  and ethanol present electron donor behavior on the graphene surface. This results were recently confirmed through theoretical calculations [14]. Therefore, by studying the doping species in a controlled way, it is possible to access how specific chemical species perturb the graphene electronic band structure and how this impact their physical properties such as magneto-optical and transport behavior [10, 12]. In addition, the minimum conductivity problem in graphene is a typical phenomenon of zero band gap electronic structure, and this has introduced drawbacks for developing a

graphene-based electronics. Carbon ribbons have been proposed as one of the solution for the minimum conductivity problem because in general its band structure exhibits a gap [15]. The gap engineering can be also achieved through doping (covalent functionalization) the graphene layer with chemical species [17] since the doping can induce a gap opening because of the breaking of translational symmetry. Therefore, the gap engineering in graphene is a hot topic and this has been exploited either by changing the geometry of ribbons or by interaction with substrate.[15, 16] The possibility of induce a gap in graphene through chemical doping has not yet been exploited.

In this work, the electronic properties of a single graphene layer interacting with  $\text{CrO}_3$  molecules are analyzed through *ab initio* based calculations and we predict that is possible to get both gap opening and spin polarization by this functionalization process. A single graphene layer is a unique system regarding the surface to volume ratio because it is solely surface and this opens up the possibility of using  $\text{CrO}_3$  intercalated graphene systems for the oxidation of primary alcohols. Our calculations shown that  $\text{CrO}_3$  molecule (a model for strongly oxidizing molecules) chemically binds to graphene surface and the electronic properties of the original graphene are modified by charge transfer from graphene to this molecule leading the  $\text{CrO}_3$  molecule act as an electron acceptor with a similar behavior observed and predicted for  $\text{CrO}_3$  interacting with single-wall carbon nanotubes (SWNT) [18]. The effect of curvature on the adsorption of this molecule on carbon hexagonal lattice is also discussed.

First principles density functional theory has been employed to investigate electronic and structural properties of graphene interacting with  $\text{CrO}_3$  molecule [19]. The SIESTA code is used [20, 21], which performs fully self-consistent calculations solving the spin polarized Kohn-Sham equations [22]. For the exchange and correlations terms, generalized gradient approximation with the parameterization of Perdew et al. is used [23]. The interaction between ionic cores and valence electrons is described by norm conserving pseudopotentials [24] in the Kleinman-Bylander form [25]. The Kohn-Sham orbitals are represented with a linear combination of pseudoatomic orbitals with a double zeta basis set plus polarization function [21]. A cutoff of 200 Ry for the grid integration is used to represent the charge density. A  $5 \times 5 \times 1$  Monkhorst-Pack grid is employed for the Brillouin zone integration, which was shown to represent correctly their properties for the present system [26].

The periodic boundary conditions and a supercell approximation are used. The supercell

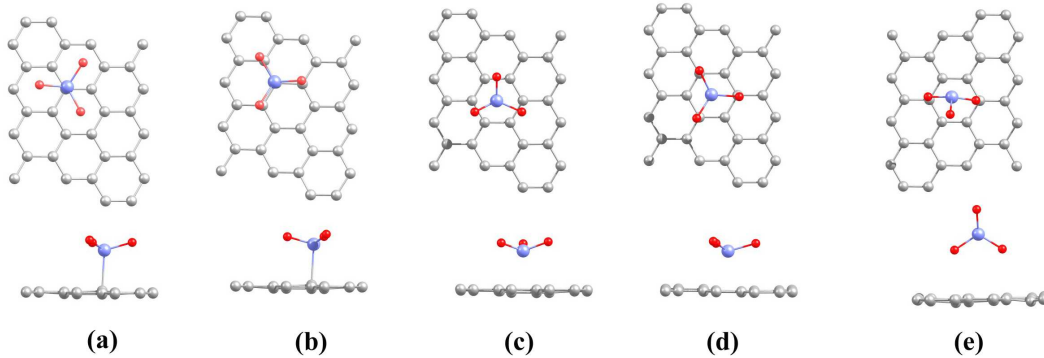


FIG. 1: Top and side view of the most stable configurations for the  $\text{CrO}_3$  interacting with graphene layer.

has 32 carbon atoms for a single graphene surface in a hexagonal lattice. The structural optimizations were performed using a conjugated gradient procedure and atomic positions of the structure are relaxed until all the force components are smaller than  $0.05 \text{ eV}/\text{\AA}$ .

Different configurations of  $\text{CrO}_3$  approaching to the graphene layer were considered in our calculations and the most stable arrangements are shown (top and side view) in Fig. 1(a)-(e). The configuration showed in Fig.1 (a) was predicted to be the most stable, with a Cr-C distance of about  $2.32 \text{ \AA}$ , while in the configuration showed in Fig.1 (e) O-C bond length is about  $2.95 \text{ \AA}$ . In Table 1 we list the closest distances Cr-C and O-C for the different configurations showed in the Figure 1.

The binding energies ( $E_B$ ) for the studied systems are calculated using the basis set superposition error (BSSE) [27]. This correction is done through the counterpoise method using "ghost" atoms, as the following equation

$$E_B = -[E_T(\text{graphene} + \text{CrO}_3) - E_T(\text{graphene}_{ghost} + \text{CrO}_3) - E_T(\text{graphene} + (\text{CrO}_3)_{ghost})], \quad (1)$$

where  $E_T(\text{graphene} + \text{CrO}_3)$  is the total energy of the system. The "ghost" molecule/graphene corresponds to additional basis wave functions centered at the position of the  $\text{CrO}_3$  molecule or the single layer graphene, but without any atomic potential.

The binding energies obtained for the different adsorption sites of  $\text{CrO}_3$  on the graphene surface are listed in Table I. These results pointed out to a physical or chemical interaction

TABLE I: Binding energies ( $E_B$ ), minimal distances and charge transfer calculated for different adsorption sites of  $\text{CrO}_3$  on graphene layer as shown in Figure 1. The minus sign in the charge transfer indicates that the  $\text{CrO}_3$  molecule receive electronic charge.

Configuration	$E_B$ (eV)	d(Cr-C) $\text{\AA}$	d(O-C) $\text{\AA}$	Charge Transfer to $\text{CrO}_3$ ( $e$ )
Fig. 1(a)	1.01	2.32	-	-0.17
Fig. 1(b)	0.91	2.33	-	-0.15
Fig. 1(c)	0.56	2.80	-	-0.11
Fig. 1(d)	0.49	2.82	-	-0.10
Fig. 1(e)	0.25	-	2.95	-0.20

between  $\text{CrO}_3$  and graphene strongly dependent on the interaction site. The transition metal atom (Cr) is preferentially bonded to the carbon atom of the graphene layer promoting an  $sp^3$ -like hybridization of the carbon atom from the graphene surface. The Mülliken population was analyzed and used for all studied configurations to predict the electronic charge transfer from the graphene surface to the  $\text{CrO}_3$  molecule. The graphene carbon atoms transfer  $0.17e$  and  $0.20e$  for the  $\text{CrO}_3$  molecule on the (Fig.1 (a)) and (Fig.1 (e)) configurations, respectively. The charge transfer on these cases occurs due to the chemical or physical adsorption of the Cr or O atoms with the carbon atoms of the graphene layer as observed on the binding energies values. We should point out that the Mülliken population does not supply a trustworthy number to charge transfer, but it indicates the trend and correct order of the charge transfer process. Then, the  $\text{CrO}_3$  molecule behaves as an electron acceptor when interacting with the graphene layer similar to what was observed for  $\text{CrO}_3$  adsorption on SWNT surface [18].

The calculated electronic band structures are presented for the pristine single graphene layer (Fig. 2(a)) and for  $\text{CrO}_3$  adsorbed on graphene (Fig.2 (b), (c), and (d)) in the most stable configurations showed in Figs.1 (a), (c) and (e)). It is clear that the  $\text{CrO}_3$  adsorption sites and orientation of the molecules affects the electronic properties of graphene being more pronounced for the adsorption sites showed in (Fig.1 (a)). The binding of  $\text{CrO}_3$  molecule lifts the degeneracy of the band crossing close to the Fermi level, thus inducing a gap opening

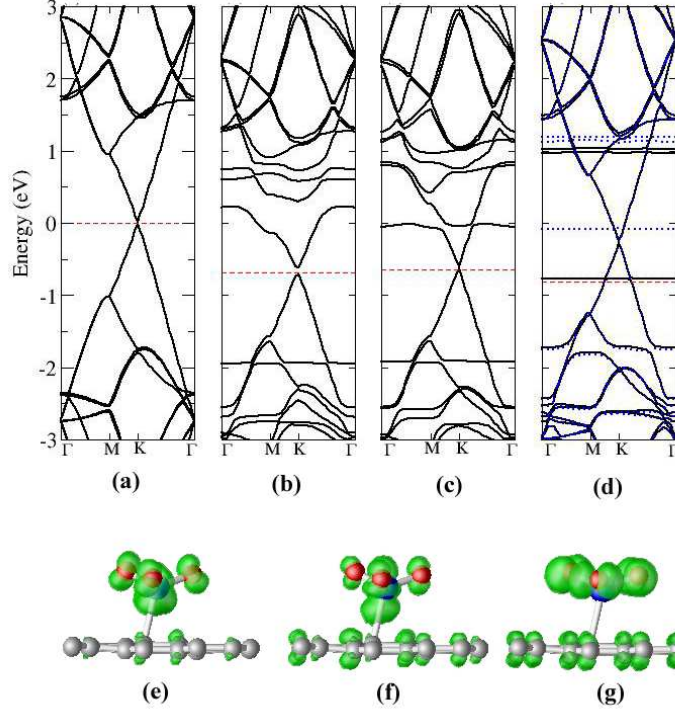


FIG. 2: Electronic band structures for (a) pristine and for different configurations of  $\text{CrO}_3$  adsorbed on graphene single layer (b), (c) and (d) that correspond to the configurations showed in Fig.1(a), (c), and (e), respectively. The (d) case has the filled and dotted lines corresponding, respectively, to the majority and minority spin levels. The horizontal dashed lines correspond to the Fermi energy. The (e), (f) and (g) show the plots for the charge isosurface for  $\text{CrO}_3$  interacting with graphene in electronic configuration presented in (b), for levels located around 0.8, -1.2 and -1.8 eV, respectively.

of about 0.12 eV at the Dirac point, which connects the valence and conduction bands at the zone edge. This gap opening is due to the breaking of graphene mirror symmetry. For the configuration shown in the Fig.1(b) the electronic behavior is similar to the Fig.2(b). In contrast, for the other configurations (Fig.1 (c)), Fig.1(d) and (Fig.1 (e)) the band crossing is preserved leaving the system semimetal at 0 K. For the (Fig.1(c)) configuration the system remains metallic (see (Fig. 2c)), with dispersionless levels of the  $\text{CrO}_3$  molecule on the valence and conduction bands. In the case (Fig.2 (d)) the majority (solid lines) and minority (dotted lines) carriers coming from 3d-Cr levels are non-degenerated and located on the valence and conduction band. Comparing the adsorption we observe that the most stable

adsorption site changes the electronic properties due to the high hybridization between the molecule and graphene levels. It is also interesting to observe the downshift of the Fermi level resulting from the charge transfer from the graphene to the  $\text{CrO}_3$  molecule. This shift relative to the pristine graphene is approximately 0.69, 0.64 and 0.8 eV showed in (Fig. 2(b)), (Fig. 2(c)), and (Fig. 2(d)), respectively. From all the studied configurations only the site with the  $\text{CrO}_3$  adsorbed on the graphene surface, as showed on the (Fig. 1(e)), presents spin polarization of  $0.4 \mu_B$ . This spin polarization can be understood in terms of redistribution of the electronic charge due to the interaction of the O atoms of the  $\text{CrO}_3$  molecule and the graphene surface. In this case, a flat electronic level is located near the Fermi level (Fig. 2(d)) that is characteristic of the  $\text{CrO}_3$  molecule.

In Fig. 2(e),(f) and (g) the plots for the localized density of states (LDOS) of  $\text{CrO}_3$  adsorbed on the graphene surface for the most stable configuration (showed in Fig. 1(a)) are presented for the electronic levels located about 0.8, -1.2 and -1.8 eV, respectively. From these LDOS plots we observe the hybridization of the molecule levels with the carbon levels from the graphene layer. This hybridization state is reflected in both binding energies and charge transfers values.

By Comparing the adsorption of the  $\text{CrO}_3$  molecule on graphene with adsorption on (8,0) SWNT surfaces [18], it is observed that the curvature effect is a crucial point to increase the adsorption of  $\text{CrO}_3$  on the carbon hexagonal lattice. The binding energy increase by 0.4 eV for the molecule adsorbed on the inner or outer surface of the nanotube (1.4 eV for both configurations) compared with the most stable configuration on the graphene surface (1.01 eV). This effect is relevant when is considered the real curved configuration (ripples) of the graphene layers [8], which will increase the efficiency of the molecule adsorption on the hexagonal carbon structures depending of the local curvature parameters.

In summary, the electronic properties of the  $\text{CrO}_3$  molecule adsorbed on the graphene single layer were analyzed through first principles calculations. It is observed that the electronic properties and the charge transfer process are very sensitive to the  $\text{CrO}_3$  adsorption site and also to the orientation of the molecule. This behavior is different from what was predicted Leenaerts et al. [14] for other molecules, where the interaction is not very sensitive to the adsorption site being only dependent on the molecule orientation with respect to the graphene surface. The  $\text{CrO}_3$  molecule interacts through a chemisorption or physisorption regime on the graphene surface depending on the adsorption site, indicating possible routes

for the use doped graphene layer as platform for carbon-based electronics since it is possible to engineer the gap and overcome the minimum conductivity problem. Furthermore, the sensitivity of electronic structure towards doping makes the graphene a potential material for chemical sensors owing to their exceptionally high surface to volume ratio.

The authors thanks A. H. Castro Neto and B. Uchoa for the valuable discussions. The authors also acknowledge CENAPAD-SP for computer time and financial support from Brazilian agencies CNPq, FAPERGS (Grants 0511570/05 and 05/2096.2) and FUNCAP (Grant 350220/2006-9). S.B.Fagan acknowledges the Brazilian Woman in Science/2006 grant from Loreal/Paris.

- 
- [1] M. S. Dresselhaus, G. Dresselhaus, P. Avouris, Carbon Nanotubes, Springer, Berlin, 2001.
  - [2] M.S. Dresselhaus and G. Dresselhaus, Adv. Phys. **51**, 1 (2002).
  - [3] P. R. Wallace, Phys. Rev. **71**, 622 (1947).
  - [4] K. S. Novoselov et al., PNAS **102**, 10451 (2005).
  - [5] K. S. Novoselov et al., Science **306**, 666 (2004).
  - [6] K. S. Novoselov et al., Nature **438**, 197 (2005).
  - [7] Y. Zhang, et al., Nature **438**, 201 (2005).
  - [8] A. K. Geim and K. S. Novoselov, Nature Mat. **6**, 183 (2007).
  - [9] E. W. Hill et al.,IEEE Trans. Magn. **42** 2694 (2006).
  - [10] F. Schedin et al., Nature Materials **6**, 652 (2007).
  - [11] N. M. R. Peres, F. Guinea and A. H. Castro Neto, Phys. Rev. B **73**, 125411 (2006).
  - [12] B. Uchoa and A. H. Castro Neto, Phys. Rev. Lett. **98**, 146801 (2007).
  - [13] S. V. Morozov et al., cond-mat/cond-mat 0703390.
  - [14] O. Leenaerts, B. Partoens, F. M. Peeters, cond-mat/cond-mat 07101757.
  - [15] J. Nilsson et al., Phys. Rev. B **76**, 165416 (2007).
  - [16] S. Y. Zhou et al., Nature Materials **6**, 770 (2007).
  - [17] T. Ohta et al., Science **313**, 951 (2006).
  - [18] S. B. Fagan et al., Chem. Phys. Lett. **406**, 54 (2005).
  - [19] P. Hohenberg and W. Kohn, Phys. Rev. **136**, 864B (1964).
  - [20] P. Ordejón and J.M. Soler, Phys. Rev. B **53**, 10441 (1996).



- [21] E. Artacho et al., Phys. Status Solidi B **215**, 809 (1999).
- [22] W. Kohn and L.J. Sham, Phys. Rev. **140**, 1133A (1965).
- [23] J. P. Perdew, E. Burke and M. Ernzenhof, Phys. Rev. Lett. **77**, 3865 (1996).
- [24] N. Troullier and J.L. Martins, Phys. Rev. B **43**, 1993 (1991).
- [25] L. Kleinman and D. M. Bylander, Phys. Rev. Lett. **48**, 1425 (1982).
- [26] H. J. Monkhorst and J. D. Pack, Phys. Rev. B **13**, 5188 (1976).
- [27] S. F.Boys and F. Bernardi, Mol. Phys. **19**, 553 (1970).